UC Davis
UC Davis Previously Published Works

Title

Acute suppression of insulin resistance-associated hepatic miR-29 in vivo improves glycemic control in adult mice

Permalink

https://escholarship.org/uc/item/6gb2n71n

Journal

Physiological Genomics, 51(8)

ISSN

1094-8341

Authors

Hung, Yu-Han
Kanke, Matt
Kurtz, C Lisa
et al.

Publication Date

2019-08-01

DOI

10.1152/physiolgenomics.00037.2019

Peer reviewed

RESEARCH ARTICLE | *Comparative, Statistical and Computational Genomics and Model Organism Databases*

Acute suppression of insulin resistance-associated hepatic miR-29 in vivo improves glycemic control in adult mice

Yu-Han Hung,[1]* Matt Kanke,[1]* C. Lisa Kurtz,[2] Rebecca Cubitt,[1] Rodica P. Bunaciu,[1] Ji Miao,[3] Liye Zhou,[4] James L. Graham,[5] M. Mahmood Hussain,[4] Peter Havel,[5] Sudha Biddinger,[3] Phillip J. White,[6] and Praveen Sethupathy[1]

[1]*Department of Biomedical Sciences, Cornell University, Ithaca, New York;* [2]*Department of Genetics, University of North Carolina, Chapel Hill, North Carolina;* [3]*Division of Endocrinology, Boston Children's Hospital, Harvard Medical School, Boston, Massachusetts;* [4]*Diabetes and Obesity Center, NYU Winthrop Hospital, Mineola, New York;* [5]*Department of Nutrition, University of California, Davis, California; and* [6]*Duke Molecular Physiology Institute, Duke University, Durham, North Carolina*

Hung YH, Kanke M, Kurtz CL, Cubitt R, Bunaciu RP, Miao J, Zhou L, Graham JL, Hussain MM, Havel P, Biddinger S, White PJ, Sethupathy P. Acute suppression of insulin resistance-associated hepatic miR-29 in vivo improves glycemic control in adult mice. *Physiol Genomics* 51: 379–389, 2019. First published June 28, 2019; doi:10.1152/physiolgenomics.00037.2019.—MicroRNAs (miRNAs) are important posttranscriptional regulators of metabolism and energy homeostasis. Dysregulation of certain miRNAs in the liver has been shown to contribute to the pathogenesis of Type 2 diabetes (T2D), in part by impairing hepatic insulin sensitivity. By small RNA-sequencing analysis, we identified seven hepatic miRNAs (including miR-29b) that are consistently aberrantly expressed across five different rodent models of metabolic dysfunction that share the feature of insulin resistance (IR). We also showed that hepatic miR-29b exhibits persistent dysregulation during disease progression in a rat model of diabetes, UCD-T2DM. Furthermore, we observed that hepatic levels of miR-29 family members are attenuated by interventions known to improve IR in rodent and rhesus macaque models. To examine the function of the miR-29 family in modulating insulin sensitivity, we used locked nucleic acid (LNA) technology and demonstrated that acute in vivo suppression of the miR-29 family in adult mice leads to significant reduction of fasting blood glucose (in both chow-fed lean and high-fat diet-fed obese mice) and improvement in insulin sensitivity (in chow-fed lean mice). We carried out whole transcriptome studies and uncovered candidate mechanisms, including regulation of DNA methyltransferase 3a (*Dnmt3a*) and the hormone-encoding gene Energy homeostasis associated (*Enho*). In sum, we showed that IR/T2D is linked to dysregulation of hepatic miR-29b across numerous models and that acute suppression of the miR-29 family in adult mice leads to improved glycemic control. Future studies should investigate the therapeutic utility of miR-29 suppression in different metabolic disease states.

Enho; insulin resistance; liver; microRNA-29 (miR-29); UCD-T2DM

INTRODUCTION

Insulin resistance (IR) is a key feature of the pathophysiological process that underlies the development of classical Type 2 diabetes (T2D), which is a complex metabolic disease influenced by both environmental and genetic factors. MicroRNAs (miRNAs) are important posttranscriptional regulators of gene expression that have been implicated in pathways underpinning T2D etiology in multiple organs including the pancreas (2, 31, 39), liver (9, 26, 44), adipose tissue (42, 44, 49), and skeletal muscle (32, 36, 43).

Accumulating evidence suggests that the dysregulation of particular hepatic miRNAs contributes to IR/T2D and that rescue of their expression can reverse disease phenotypes. In 2011, Trajkovski and colleagues (44) reported that hepatic miR-103/107 is aberrantly elevated in the liver of high-fat diet (HFD)-fed obese mice as well as in leptin-deficient *ob/ob* mice. In the same study, they showed that treatments of anti-miRNA-oligonucleotides targeting miR-103/107 attenuate hyperglycemia in part through improvement in hepatic insulin signaling. This possible treatment approach garnered broad attention and entered Phase I clinical trials for patients with hepatic steatosis and T2D. In 2013, the same group reported a significant upregulation of another hepatic miRNA, miR-802, in mice fed HFD and in *db/db* mice, which carry a homozygous missense mutation in the leptin receptor. In addition, they showed that systemic administration of locked nucleic acid (LNA) inhibitors of miR-802 to HFD-fed mice significantly improves glucose tolerance, in part due to increased levels and activity of Hepatocyte nuclear factor 1b (Hnf1b), which leads to improved systemic insulin sensitivity (26). Also in 2013, another group showed that tail vein injection of anti-sense oligonucleotides targeting miR-34a, which is remarkably elevated in the liver of HFD-fed mice, helped to recalibrate the hepatic levels of Sirtuin 1 (Sirt1) and thereby improve glucose tolerance and IR (9). Taken together, the findings from these preclinical animal studies suggest that multiple hepatic miRNAs contribute to the impairment of hepatic insulin signaling and represent candidate therapeutic targets for T2D. However, these miRNAs were identified only in certain models of IR/T2D and whether their

dysregulation is shared across other models has not been evaluated. In addition, it is still unknown how many other liver miRNAs may be involved in the control of insulin sensitivity.

This study provides new insight into family members of miR-29 (miR-29a, b, and c) in the liver as modulators of insulin sensitivity in the fasted state, in addition to their roles that we previously reported as regulators of circulating lipids during the fed state (29). First, using a sequencing-based approach to characterize liver miRNA profiles, we identified a group of seven miRNAs that are consistently dysregulated across five well-established but very different rodent models of IR/T2D, including *db/db* mice, streptozotocin (STZ)-treated mice, and *fa/fa* Zucker Fatty (ZF) rats. Among these seven, we identified that miR-29b is the most strongly associated with T2D progression in an independent rat model of adult-onset diabetes, UCD-T2DM, and that its levels are attenuated by treatments known to improve IR in rodent and rhesus macaque models. Importantly, we then applied LNA technology in vivo to demonstrate that acute suppression of the miR-29 family lowers fasting glucose in chow-fed lean as well as HFD-induced obese mice. Whole transcriptome studies revealed potential underlying mechanism involving the hormone-encoding gene energy homeostasis associated (*Enho*). Overall, this study shows that aberrant elevation of miR-29b in the liver is common across multiple models of IR/T2D and demonstrates that acute suppression of the miR-29 family exerts beneficial effects for glycemic control in adult mice.

MATERIALS AND METHODS

Animal models. Four male rodent models of IR/T2D were included in this study for profiling miRNAs in the liver. They include: *1) ob/ob* mice: 2 mo old obese mice ($n = 5$) and lean control ($n = 5$); *2)* STZ-injected mice: 2 mo old C57BL/6J mice injected with 180 mg/kg dose of STZ ($n = 5$) and control mice injected with saline ($n = 5$); *3) fa/fa* Zucker Fatty (ZF) rats: 5.5 mo old obese rats ($n = 5$) and lean control ($n = 5$); and *4)* UCD-T2DM rats: 6 mo old rats in prediabetic condition ($n = 3$), 6 mo old rats with T2DM for 2 wk ($n = 6$), 6 mo old rats with T2DM for 3 mo ($n = 3$), and 9 mo old rats with T2DM for 6 mo ($n = 5$).

Two models of IR/T2D were used for assessing miRNA changes in the liver after receiving treatments (3, 48). They include: *1)* male 3 mo old *fa/fa* rats receiving daily treatment of 3,6-dichlorobrenzo(b)thiophene-2-carboxylic acid (48) (BT2, 20 mg/kg intraperitoneally) ($n = 5$) and vehicle ($n = 5$) for 1 wk, and *2)* male 10–20 yr old rhesus macaques chronically fed with high-fat diet/high-fructose syrup with daily supplementation of fish oil ($n = 3$) or sunflower oil control ($n = 3$) for 4 wk. As previously described in (3), the fish oil (16% EPA/11% DHA; 32.1% n-3 fatty acids; 2.4% n-6 fatty acids; 77.3% total fatty acids; Jedwards International, validated by Covance) was mixed into a treat such as ice cream, yogurt, jelly, applesauce, or pudding; and 1% by weight of egg powder was added to make an emulsion. Then, 44 g of the mixture containing 4 g of fish oil was provided to the monkeys each day. The control monkeys received the same mixture with 4 g of safflower oil [0.05% free fatty acids; 6.54% palmitic acid (16:0); 2.62% stearic acid (18:0); 14.97% oleic acid (18:1); 73.47% linoleic acid (18:2); 0.05% linolenic acid (18:3); 0.15% behenic acid (22:0); Jedwards International] instead of fish oil.

All animal procedures were performed with the approval and authorization of the Institutional Animal Care and Use Committee (IACUC) at each participating institution.

In vivo LNA study. To evaluate the short-term effects of LNA29 in adult normoglycemic mice, C57BL/6J mice (female 9–11 wk old) fed chow-diet (Lab Diet 5047) were used. To evaluate the short-term effects of LNA29 in adult mice with diet-induced IR phenotype, C57BL/6J mice (male 9–11 wk old) were fed with HFD (45% kcal from fat; Research Diets D12451) for 4 wk before receiving LNA treatments. The mice enrolled in the in vivo LNA studies were maintained on a 12 h light/dark cycle with access to diet and water ad libitum. Animals received one dose of subcutaneous injection of *1)* RNase-free sterile saline (BioO Scientific, Austin, TX), *2)* LNAs against scrambled sequences (Qiagen), or *3)* LNAs against mmu-miR-29a-3p (5′-ATTTCAGATGGTGCT-3′) and mmu-miR-29bc-3p (5′-ATTTCAAATGGTGCT-3′) at 20 mg/kg each (Qiagen). In mice, there are two miR-29 loci (miR-29a/b-1 locus on chromosome 6qA3.3 and miR-29b-2/c locus on 1qH6), which together produce three miR-29 family members (miR-29a, b, c). The mature sequences of the miR-29 family members have an identical seed sequence AGCACC and are conserved across humans, rats, and mice (27). During the study, blood was collected via submandibular or tail vein. For tissue collection, the animals were overnight fasted and anesthetized at *day 7* postdose of LNA. Various tissues including the liver were harvested and flash-frozen in liquid nitrogen and stored at −80°C for further analysis. For assessing insulin sensitivity, oral glucose tolerance test (OGTT) and insulin sensitivity test (IST) were performed at *day 5* and *7* postdose of LNA, respectively. The in vivo LNA study was carried out multiple times across two institutions, NYU Winthrop Hospital and Cornell University. All animal procedures were performed with the approval and authorization of the IACUC at each participating institution.

Insulin sensitivity assays. In the OGTT, mice were fasted overnight and blood was taken from the tail vein for measurements of basal levels of blood glucose (0 min) by glucometer. Followed by an oral gavage of dextrose (2 g/kg), blood glucose was determined at 30, 60, 90, and 120 min postgavage. In the IST, mice were fasted for 2 h and the blood was taken from the tail vein for measurements of basal levels of blood glucose (0 min). Followed by an intraperitoneal injection of Humulin-R insulin (0.6 U/kg) (CUHA Pharmacy), the blood glucose was determined at 15, 30, 60, and 90 min postinsulin injection. In the IST experiments, two saline mice and two LNA-scramble (LNAscr)-treated mice did not exhibit any reduced blood glucose at the 15 min time point or had even higher glucose levels compared with basal levels in response to the insulin injection, which indicates nonresponsiveness to insulin likely due to human error in the intraperitoneal injection. Thus, the measurements from these mice were entirely excluded from the analysis.

RNA extraction and real-time quantitative PCR. Total RNA was isolated using the Total RNA Purification kit (Norgen Biotek, Thorold, ON, Canada). High Capacity RNA to cDNA kit (Life Technologies, Grand Island, NY) was used for reverse transcription of RNA. TaqMan microRNA Reverse Transcription kit (Life Technologies) was used for reverse transcription of miRNA. Both miRNA and gene expression quantitative (q)PCR were performed using TaqMan assays (Life Technologies) with either TaqMan Universal PCR Master Mix (miRNA qPCR) or TaqMan Gene Expression Master Mix (mRNA qPCR) per the manufacturer's protocol, on a Bio-Rad CFX96 Touch Real Time PCR Detection System (Bio-Rad Laboratories, Richmond, CA). Reactions were performed in triplicate using either *U6* (miRNA qPCR) or *Rps9* (mRNA qPCR) as the normalizer.

Small RNA library preparation and sequencing. The small RNA sequencing of fasted liver samples from all the models enrolled in this study was conducted at the Genome Sequencing Facility of Greehey Children's Cancer Research Institute at University of Texas Health Science Center at San Antonio, TX. Libraries were prepared using the TriLink CleanTag Small RNA Ligation kit (TriLink Biotechnologies, San Diego, CA) and sequenced on the HiSeq2500 platform with single-end 50 bp sequencing depth. Raw sequencing data and miRNA quantification tables can be accessed through Gene Expression Omnibus (GEO) record GSE122044.

RNA library preparation and sequencing. RNA-sequencing libraries of the liver from fasted LNA29-treated C57BL/6J mice were

prepared with the Illumina TruSeq polyA+ Sample Prep Kit. Sequencing was carried out on the Illumina HiSeq2000 platform with single-end 100 bp sequencing depth at the UNC High Throughput Sequencing Core Facility. Raw sequencing data as well as normalized counts are available through GEO accession GSE122044.

Bioinformatics analysis. The small RNA-sequencing reads were aligned to mouse genome (mm10) for mouse samples, rat genome (rn6) for rat samples, or human genome (hg19) for monkey samples and quantified with miRquant 2.0 as previously described (22), with the exception that raw miRNA counts were normalized with DESeq2 (35) to determine significance. MiRNA annotation was performed with miRbase (r18), and the resulting data are presented in this study. MiRNA annotation of just the mouse samples was also reperformed with the newer release of miRbase (r22), and the data are consistent with the data generated with miRbase r18. MiRNA binding site enrichment among differentially expressed genes was determined by miRhub (1). The microarray study of hepatic miRNA profiles of HFD-fed C57BL/6J mice, published by Kornfeld et al. (26), was used to intersect with our miRNA profiles of multiple rodent models of hepatic IR. In Kornfeld et al. (26) miRNA expression levels were quantified by using the Rodent TaqMan Array microRNA Cards A and B (Applied Biosystems), which cover 674 murine miRNAs and small nucleolar RNAs (as appropriate controls). The data are presented with *P* values (two-tailed unpaired Student's *t*-test) and fold-changes of HFD relative to control chow diet. RNA-sequencing reads were mapped to genome release with rn6 STAR (v2.5.3a) (12), and transcript quantification was performed with Salmon (v0.6.0) (38). Differential gene expression analysis was accomplished by using DESeq2 (35).

Cell culture and luciferase assays. For testing changes in *Enho* expression by LNA29, Huh7 cells were maintained in 25 mM glucose DMEM (Sigma-Aldrich) supplemented with 10% FBS, 2 mM L-glutamine, 1 mM sodium pyruvate, and nonessential amino acids and cultured in a humidified incubator at 37 °C and 5% CO_2. Transfection was performed by using Lipofectamine 2000 (Life Technologies). Huh7 cells were treated with transfection reagent alone or 200 nM of miRIDIAN microRNA hsa-miR-29a-3p inhibitor (Dharmacon). After 48 h, the cells were lysed for RNA isolation. For luciferase assays, HEK293T cells were maintained in 25 mM glucose DMEM (Sigma-Aldrich) supplemented with 10% FBS and 2 mM L-glutamine (Invitrogen, Grand Island, NY) and cultured in a humidified incubator at 37 °C and 5% CO_2. HEK293T cells were seeded into 24-well plates and allowed to grow to reach 70% confluence. The cells were then transfected with the following conditions *1*): 200 ng of pEZX-MT01 empty vector alone, *2*) 200 ng of vector containing 3′-untranslated region (UTR) of *ENHO* (GeneCopoeia, Rockville, MD) alone, *3*) 200 ng of vector containing 3′-UTR of *ENHO* and 10 nM miRIDIAN microRNA hsa-miR-29a-3p mimic (5′-UAGCACCAUCUGAAAU-CGGUUA- 3′, Dharmacon), or *4*) 200 ng of vector containing 3′-UTR of *ENHO* and 10 nM LNAs against miR-29a (5′-ATTTCA-GATGGTGCT-3′, Qiagen). Transfection was performed with Lipofectamine 2000 (Life Technologies). After 48 h, the cells were lysed and luciferase activity was measured with the Luc-Pair luciferase assay kit (Agilent, Santa Clara, CA) on a GloMax 96 Microplate Luminometer (Promega, Madison, WI).

Statistics. The quantitative data are reported as an average of biological replicates ± standard error (SE) of the mean. Unless indicated otherwise, statistical differences were assessed by two-tailed Student's *t*-test with threshold *P* value < 0.05.

RESULTS

Seven dysregulated hepatic miRNAs are shared across multiple different rodent models of IR/T2D. To identify liver miRNAs that are strongly connected to IR/T2D, we first performed small RNA sequencing on total RNA isolated from the livers of three IR/T2D models (*ob/ob* mice, STZ mice, and

fa/fa ZF rats) and identified significantly dysregulated miRNAs that are shared across the models. As expected, the overall hepatic miRNA profile of each model was distinct (Fig. 1, *A–C*; Supplementary Fig. S1, *a–c*). (Supplementary materials can be found at https://github.com/Sethupathy-Lab/2019_AJP-GI_Hung_et_al_supplementary_material/tree/v1.1.0.) Varying numbers of miRNAs were significantly (fold-change > 1.5, *P* < 0.05) altered when compared with matching controls (Fig. 1, *A–C*). *Ob/ob* mice had 145 differentially expressed miRNAs (68 down, 77 up) compared with lean controls (Fig. 1, *D* and *E*). STZ mice had 90 differentially expressed miRNAs (26 down, 64 up) compared with saline-treated controls (Fig. 1, *D* and *E*). ZF rats had 130 differentially expressed miRNAs (8 down, 122 up) compared with lean controls (Fig. 1, *D* and *E*). Remarkably, among the downregulated miRNAs, none were shared across all three models (Fig. 1*D*). In contrast, there were 16 shared upregulated miRNAs (Fig. 1*E*).

Next, we assessed the expression levels of each of these 16 miRNAs with publicly available liver microarray data for miRNAs from two additional IR/T2D models, *db/db* mice and HFD-fed C57BL/6 mice (26). We found that seven of the 16 miRNAs are upregulated in at least one of these two additional models (Fig. 1*E*): miR-148b-3p, miR-222-3p, miR-28-5p, miR-34a-5p, miR-802-5p, miR-29b-3p, and miR-107-3p. Notably, of these seven, four are significantly upregulated across all models after multiple testing correction (miR-222-3p, miR-34a-5p, miR-802-5p, and miR-29b-3p; *P*-adjusted < 0.2). The expression levels of the seven shared upregulated miRNAs in the models of *ob/ob* mice, STZ mice, and ZF rats are shown in Fig. 1*F*. Overall, the sequencing-based analysis in the present study identified seven miRNAs that are consistently elevated across multiple IR/T2D models. Several of these seven miRNAs are in families that have been strongly connected previously to the control of insulin signaling (e.g., miR-107, miR-802, miR-34a, and miR-29a/b/c) (9, 21, 23, 26, 37, 44), obesity-related phenotypes (e.g., miR-28) (21), gluconeogenesis (e.g., miR-29a/b/c) (13, 51), and/or lipid homeostasis (e.g., miR-148, miR-222 and miR-29a/b/c) (7, 17, 29, 30, 45). Liver miRNA profiles in the rodent models with metabolic dysfunction included in the present study are provided here: https://github.com/Sethupathy-Lab/metabomir.

Hepatic miR-29b is the most strongly associated miRNA with diabetes progression in the UCD-T2DM rat model. All of the aforementioned disease models are based on single genetic mutations or single dietary/chemical interventions, and many do not lead to overt T2D (24). To determine which if any of the seven shared miRNAs identified in the aforementioned models also exhibit persistent dysregulation during the development and progression of T2D, we employed a relatively newer model developed at the University of California at Davis, called the UCD-T2DM rat (10). UCD-T2DM rats reproducibly develop adult-onset, polygenic obesity, and IR followed by a natural disease progression to overt T2D, more closely mirroring the course of classic T2D pathogenesis in humans. Small RNA sequencing was performed on the liver of UCD-T2DM rats in the prediabetic stage, 2 wk after T2D onset (2 wk), and 3 mo after T2D onset (3 mo) (Fig. 2*A*). As expected, the UCD-T2DM rats exhibited a changing miRNA landscape during disease progression (Fig. 2*B*).

We next evaluated in this model the seven dysregulated miRNAs identified in Fig. 1*E*. Unexpectedly, the expression
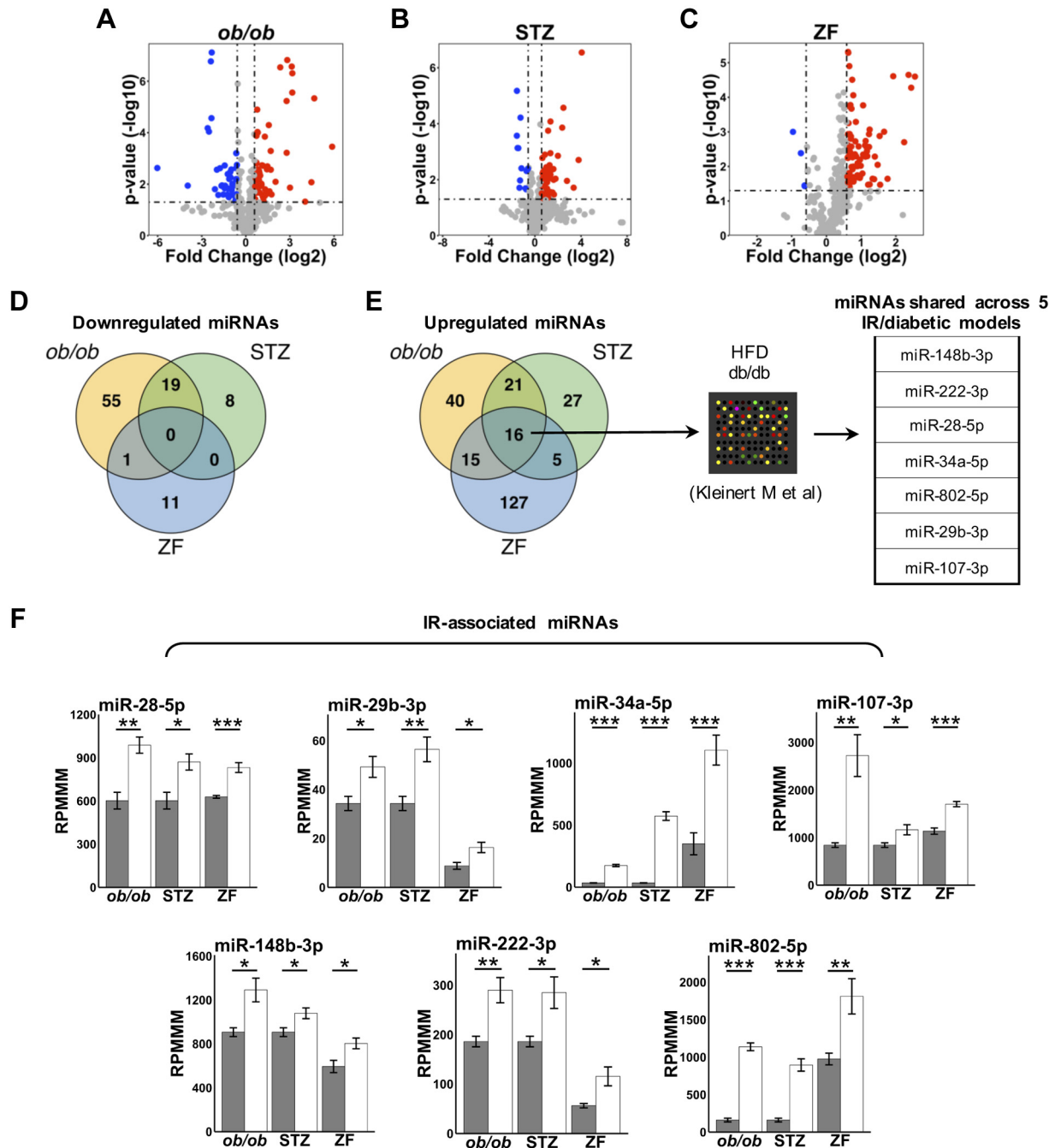
Fig. 1. Identification of a suite of liver microRNAs (miRNAs) dysregulated across multiple rodent models of insulin resistance (IR). *A–C*: volcano plots of differentially expressed miRNAs in *ob/ob* mice, STZ mice, and ZF rats relative to the matching controls. Dashed lines represent $P < 0.05$ and fold-change > 1.5. *D*: Venn diagram showing the number of shared and unique downregulated miRNAs across *ob/ob* mice, STZ mice, and ZF rats. The cutoff threshold is $P < 0.05$ (two-tailed Student's *t*-test based on RPMMM expression) and RPMMM > 20. *E*: Venn Diagram showing the number of shared and unique upregulated miRNAs across *ob/ob* mice, STZ mice, and ZF rats. The cutoff threshold is $P < 0.05$ (two-tailed Student's *t*-test based on RPMMM expression) and RPMMM > 20. The shared upregulated miRNAs were further overlaid with the list of upregulated miRNAs identified in two IR models (*db/db* and HFD mice) in the study of Kleinert et al. (24). Seven out of the 13 miRNAs were identified to be upregulated in at least one additional model and are referred to as "IR-associated miRNAs." Those among the seven miRNAs that pass multiple testing correction (*P*-adjusted < 0.2) across all of the models are miR-222-3p, miR-34a-5p, miR-802-5p, and miR-29b-3p. *F*: sequencing data showing the expression levels of the seven "IR-associated miRNAs" in models of *ob/ob* mice, STZ mice, and ZF rats. HFD, high-fat diet; RPMMM, reads per million mapped to miRNAs; STZ, streptozotocin; ZF, Zucker Fatty. *Ob/ob* mice $n = 5$ (control $n = 5$), STZ mice $n = 5$ (control $n = 5$), ZF rat $n = 5$ (control $n = 5$). *$P < 0.05$, **$P < 0.01$ and ***$P < 0.001$ by two-tailed Student's *t*-test based on RPMMM expression.
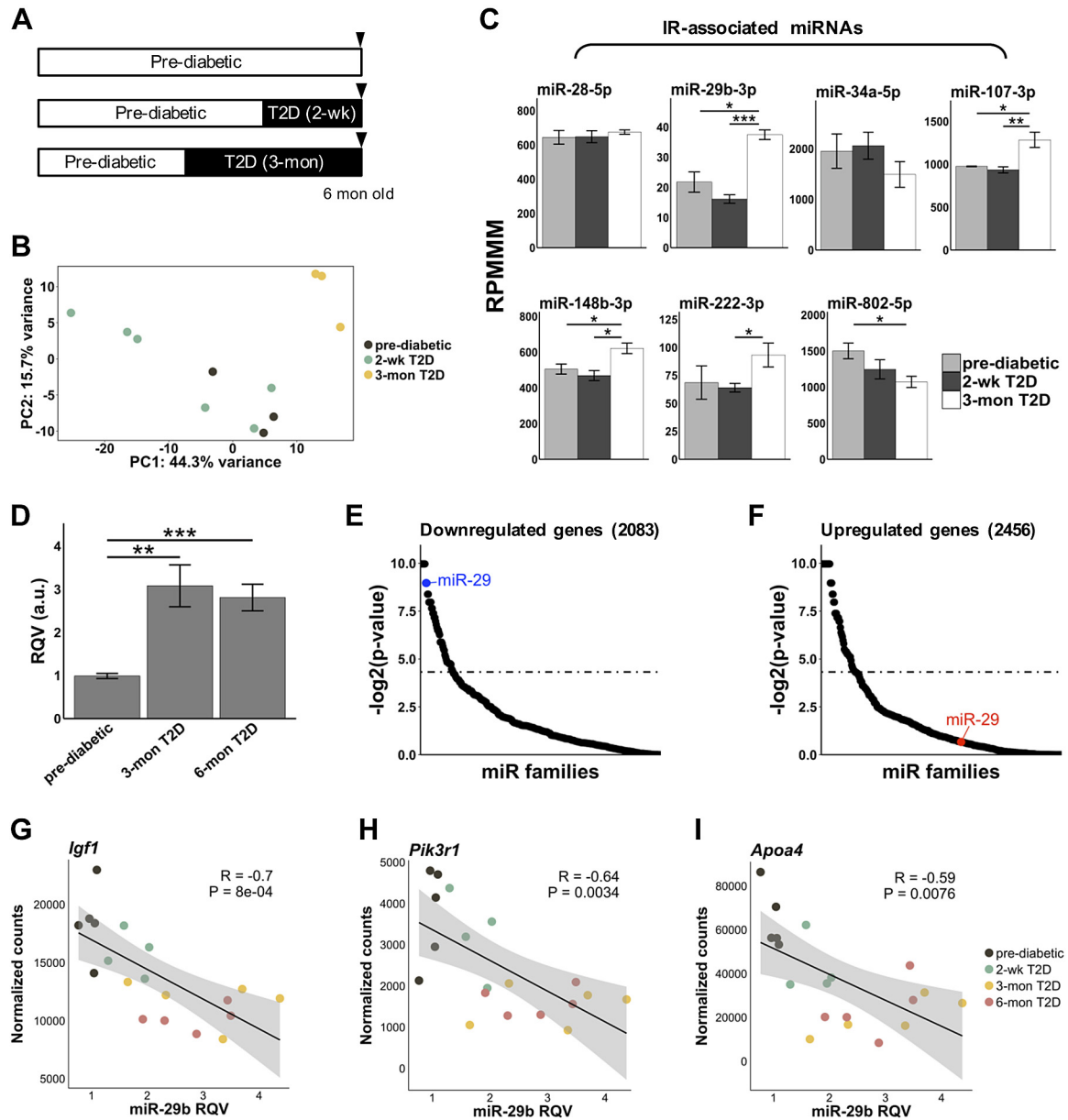
Fig. 2. The progressive dysregulation of miR-29b in the liver reflects disease progression of insulin resistance-Type 2 diabetes (IR/T2D) in UCD-T2DM rats. *A*: the experimental design of monitoring diabetes progression in UCD-T2DM rats. *B*: PCA plot of miRNA profiles in the liver of UCD-T2DM rats in the indicated group. *C*: sequencing data showing the expression levels of the seven "IR-associated miRNAs" in UCD-T2DM rats in the indicated group. RPMMM, reads per million mapped to miRNAs. *$P < 0.05$ and ***$P < 0.001$ by two-tailed Student's *t*-test based on RPMMM expression. *D*: RT-quantitative (q)PCR of hepatic miR-29b levels in prediabetic, 3 mo, and 6 mo UCD-T2DM rats. *$P < 0.05$, **$P < 0.01$ and ***$P < 0.001$ by two-tailed Student's *t*-test. Enrichment analysis of miRNA target sites (using the Monte Carlo simulation tool miRhub) in genes downregulated (*E*) and upregulated (*F*) in the liver of UCD-T2D rats with T2DM onset for 6 mo compared with prediabetic rats (dashed line represents $P = 0.05$). *G*: correlation plot of miR-29b expression levels with its validated target gene *Igf1*. *H*: correlation plot of miR-29b expression levels with its validated target gene *Pi3kr1*. *I*: correlation plot of miR-29b expression levels with *Apoa4* expression. Gray areas in the correlation plots represent the 95% confidence interval. Prediabetic rat $n = 3$, 2 wk T2D rat $n = 6$, 3 mo T2D rat $n = 3$, 6 mo T2D rat $n = 5$. RQV, relative quantification value.

level of miR-802 was significantly decreased; however, the levels of miR-107, miR-148b, miR-222, and miR-29b were significantly increased in the 3 mo T2D compared with either prediabetic or 2 wk diabetic rats (Fig. 2*C*). Among these four miRNAs that exert progressive dysregulation, miR-29b is the only one that is altered by >1.5-fold in an overt diabetes state (3 mo) relative to the prediabetic condition. To validate this observation from the sequencing analysis, we determined by real-time qPCR (RT-qPCR) the expression levels of miR-29b

in UCD-T2DM rats in the prediabetic stage, 3 mo, and 6 mo after T2D onset (Fig. 2*D*). The RT-qPCR data confirmed the results of the sequencing analysis and demonstrated that hepatic miR-29b exhibits persistent dysregulation after T2D onset (Fig. 2*D*).

To assess the impact of elevated miR-29b on the gene expression profile, we performed RNA-Seq on the livers of UCD-T2DM rats and conducted enrichment analysis for miRNA target sites with our previously described bioinformat-

ics tool, miRhub (40). We hypothesized that if the upregulation of miR-29 is functionally relevant, it should lead to the downregulation of direct target genes. Consistent with our hypothesis, the predicted target sites of the miR-29 family were significantly enriched only in the downregulated gene set, but not in the upregulated gene set, in 6 mo UCD-T2DM rats compared with prediabetic rats (Fig. 2, *E* and *F*). Expectedly, *Igf1* and *Pik3r1*, which we previously showed are upregulated by the suppression of miR-29 in the mice during the fed state (29) and have been validated as miR-29 target genes in other cell types (41, 46), are indeed negatively correlated with miR-29b levels in UCD-T2DM rats (Fig. 2, *G* and *H*). These two genes are known to be involved in the insulin signaling pathway (50). Notably, another gene, Apolipoprotein A4 (*Apoa4*), which is not a predicted miR-29 target but does encode a protein that promotes insulin sensitivity (33), was also strongly inversely correlated with miR-29, likely due to an indirect mechanism (Fig. 2*I*).

Interventions that improve insulin sensitivity lower hepatic miR-29b in rodent and primate models of diabetes. Given that the expression levels of hepatic miR-29b exhibit persistent dysregulation after T2D onset, we next asked whether hepatic miR-29b would be responsive to treatments that are known to alleviate IR. We first turned to obese, insulin-resistant ZF rats subject to a 1 wk treatment of the BT2 compound, which was recently shown to improve insulin sensitivity by inhibiting the branched chain α-keto acid dehydrogenase kinase in the liver (48). By performing small RNA-Seq on the liver of ZF rats after either vehicle (control) or BT2 treatment (Supplementary Fig. S2*a*), we found that miR-29b levels were lowered in BT2-treated ZF rats compared with vehicle-treated ZF rats,

although it did not meet statistical significance (Supplementary Fig. S2, b and c). However, miR-29b is one of only three miRNAs that is both upregulated in obese ZF compared with lean littermates and downregulated in obese ZF rats after BT2 treatment (Supplementary Fig. S2*d*). The second IR-improving treatment we examined is 4 wk of daily supplementation of fish oil in high-fructose-diet fed rhesus monkeys (3), which has been shown to effectively prevent fructose-induced IR. We performed small RNA sequencing in the liver of high-fructose diet-fed rhesus monkeys supplemented with fish oil or sunflower oil (control) (Supplementary Fig. S2*e*) and found that miR-29b levels trend lower in fish oil-treated rhesus monkeys compared with controls (Supplementary Fig. S2, *f* and *g*). Although the amplitude of the effect is modest, miR-29b does appear to be responsive to interventions that improve IR in both rodent and nonhuman primate T2D models. This further raises the possibility that suppression of miR-29b and the other members of miR-29 family, which have the same seed sequence for recognizing target genes, could lead to glycemic benefits.

Acute suppression of the miR-29 family enhances glycemic control in chow-fed lean and HFD-induced obese mice. To examine the effect of suppressing the miR-29 family (miR-29a, b, and c) on glycemic control, we conducted an in vivo study with chow-fed wild-type (WT) mice treated with one dose of locked nucleic acid inhibitors of miR-29abc (LNA29) for 1 wk (Fig. 3*A*, Supplementary Fig. S3*a*). We have previously shown that hepatic expression levels of all three miR-29 family members are effectively suppressed by LNA29 and that the hepatic levels of a validated miR-29 target gene, collagen type I alpha (*Col1a1*), are significantly upregulated by LNA29 in
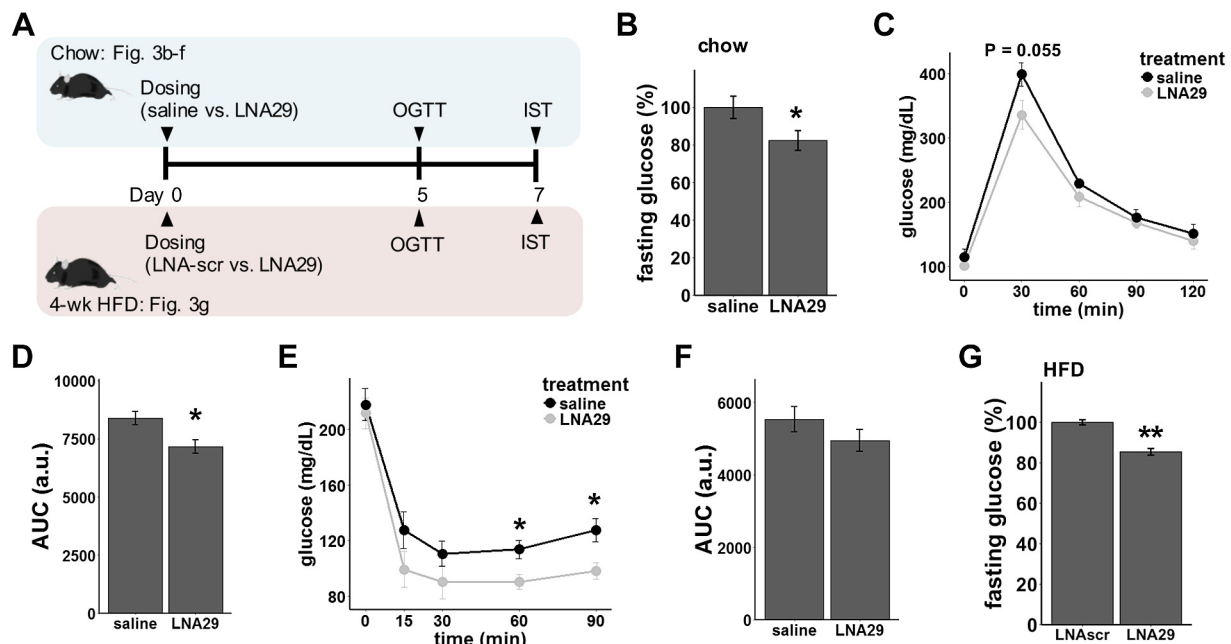

Fig. 3. Acute suppression of the miR-29 family in vivo enhances glycemic control in adult chow-fed lean as well as HFD-induced obese mice. *A*: experimental design for assessing the influence of LNA29 on systemic insulin sensitivity. *B*: overnight fasting blood glucose in saline- or LNA29-treated chow-fed lean C57BL/6J mice (saline, $n = 12$; LNA29, $n = 12$). *C*: levels of blood glucose of chow-fed lean mice in the indicated group during the time course of oral glucose tolerance test (OGTT; saline, $n = 6$; LNA29, $n = 5$). *D*: area under curve (AUC) calculated from the OGTT shown in (c). *E*: levels of blood glucose of chow-fed lean mice in the indicated group during the time course of insulin sensitivity test (IST; saline, $n = 6$; LNA29, $n = 5$). *F*: AUC calculated from the IST shown in D. *G*: overnight fasting blood glucose in LNAscr- or LNA29-treated HFD-fed lean C57BL/6J mice (LNAscr, $n = 3$; LNA29, $n = 3$). *$*P < 0.05$ and **$*P < 0.01$ by two-tailed Student's *t*-test.

the mice at *day 7* postdose. We've also shown that this treatment scheme of LNA29 leads to a significant reduction of circulating lipids during the fed state (29), but the potential beneficial effect of LNA29 on glycemic control in the fasted state has never been investigated. In the present study, a set of 9–10 wk old chow-fed lean C57BL/6J mice received one dose of either saline or LNA29, and insulin sensitivity was assessed by OGTT and IST at *day 5* and *7* postdose, respectively (Fig. 3*A*). LNA29 treatment leads to a significant reduction in overnight fasting glucose compared with saline treatment in chow-fed lean mice (Fig. 3*B*). In addition, the LNA29-treated lean mice exhibited improvements in glucose tolerance as indicated by a significant decrease in the area under the curve (AUC) of the OGTT test (Fig. 3, *C* and *D*), as well as improvements in insulin sensitivity as demonstrated by low-ered levels of blood glucose in the IST (Fig. 3, *E* and *F*) compared with saline-treated mice. Another cohort of 9–10 wk old chow-diet fed C57BL/6J mice that received one dose of LNAscr, which does not alter expression of hepatic miR-29 family (Supplementary Fig. S3*a*), exhibited no significant changes in fasting glucose levels, OGTT, or IST relative to saline treatment (Supplementary Fig. S3, *b–d*), which demon-strates that the effects on fasting glucose, OGTT, and IST are specific to LNA29. In these in vivo studies, one dose of LNA29 or LNAscr does not lead to changes in body weight in the chow-fed lean mice compared with saline treatment (Supple-mentary Fig. S3, *e* and *f*).

We next tested the acute effect of LNA29 treatment in HFD-induced obese mice (Fig. 3*A*). A set of 8–9 wk old C57BL/6J mice were fed HFD (45% kcal from fat) for 4 wk. We first confirmed that HFD-fed mice exhibit significant in-creases in body weight and IR as determined by OGTT and IST compared with age-matched chow-fed mice (Supplementary Fig. S4, *a–e*). Consistent with the observations in chow-fed mice, one dose of LNA29 treatment in the context of HFD intervention also robustly suppressed miR-29 family members and elevated levels of *Col1a1* in the liver compared with LNAscr (Supplementary Fig. S5, *g* and *h*). Although glucose tolerance did not improve by LNA29, (Supplementary Fig. S5, *i* and *j*), the LNA29-treated mice did exhibit significant reduc-tions in fasting glucose levels compared with LNAscr-treated mice (Fig. 3*G*, Supplementary Fig. S5*f*). Taken together, these observations suggest improved fasting blood glucose levels after only 1 wk of LNA29 administration in both chow-fed lean and HFD-induced obese mice, but the reasons for the different effects of LNA29 on OGTT and IST in chow-fed versus HFD-fed mice are not yet known.

LNA29-mediated improvement in insulin sensitivity occurs concomitantly with upregulation in liver expression of miR-29 target genes Dnmt3a and Enho. Though we observed a signif-icant reduction in fasting glucose by LNA29 (Fig. 3), previ-ously we did not observe an effect of LNA29 on fed glucose levels (29). This indicates that the beneficial effect of LNA29 on glycemic control is primarily in the fasted state. To identify candidate miR-29 target genes in the liver that may play a role in the LNA29-induced improvement in glycemic control, we performed RNA-Seq analysis on the liver from fasted LNA29-treated mice. We identified a total of 2,219 genes (1,091 up, 1,128 down) that are altered by LNA29 compared with saline treatment ($P < 0.05$, adjusted $P < 0.2$, base mean > 50). By performing miRhub analysis we further confirmed that the

genes that are upregulated by LNA29 are significantly enriched for predicted target sites of miR-29 (Fig. 4*A*), whereas the genes that are downregulated by LNA29 are not (Fig. 4*B*).

Among the genes upregulated by LNA29 there are 171 genes that have highly conserved predicted target sites (posi-tionally preserved in two additional species besides mouse) for miR-29 (Fig. 4*C*, Supplementary Table S1). These 171 genes include those that have been validated as targets of miR-29 (e.g., *Dnmt3a* and *Dnmt3b*) (14, 20) (Fig. 4*D*). *Dnmt3a* and *Dnmt3b* are known to encode de novo methyltransferases, and altered expression of Dnmt3a in particular has been linked to insulin sensitivity in multiple tissue/cell types such as adipose and neurons (11, 25, 52). Consistent with this, Western blotting shows a significant increase in Dnmt3a in the liver of mice treated with LNA29 compared with saline (Supplementary Fig. S5, *a* and *b*).

The 171 genes (Fig. 4*C*) also include those that have not been validated previously as targets of miR-29 but have been shown to involved in the regulation of insulin sensitivity [e.g., diacylglycerol kinase-δ (*Dgkd*) and *Enho*] (Fig. 4*D*). Dgkd was reported to contribute to insulin sensitivity through reducing intracellular diacylglycerol content in the muscle (8). *Enho* is highly expressed only in the liver and the brain and encodes the hormone Adropin, which has also been shown to regulate insulin sensitivity (16, 28). Specifically, hepatic *Enho* expres-sion is significantly reduced under chronic HFD diet in mice (28) and the whole-body knockout mice of Enho develop insulin resistance (16). Given the relevance of hepatic Enho to the regulation of glycemia and the upregulation of *Enho* in mouse livers treated with LNA29 (Fig. 4, *C–E*), we sought to examine whether *Enho* expression is regulated by miR-29 in human cells as well. We treated Huh7 cells with either trans-fection reagent alone or 200 nM inhibitor of one of the family members of miR-29 (miR-29a). We showed that *Enho* expres-sion is significantly upregulated by the suppression of miR-29a compared with mock treatment (Fig. 4*F*). To test whether *Enho* is a direct target of miR-29, we performed 3′-UTR reporter gene assays in HEK-293 cells (Fig. 4*G*). We demonstrated that the treatment with miR-29a mimics significantly decreases the activity of luciferase that is linked with the 3′-UTR of *Enho* (Fig. 4*G*). Likewise, treatment with LNA29a significantly increases luciferase activity compared with mock control (Fig. 4*G*). These findings together motivate future work to determine the extent to which miR-29 regulation of *Enho* controls insulin sensitivity.

DISCUSSION

In this study we first started with a sequencing-based ap-proach to identify the set of hepatic miRNAs (including miR-29b) that are commonly dysregulated across multiple rodent models of IR/T2D. We further demonstrated that miR-29b is the most strongly associated with disease progression in UCD-T2DM rats and that miR-29b appears to be responsive to interventions that improve IR in both rodent and nonhuman primate models of IR/T2D. Finally, we showed that in vivo suppression of the hepatic miR-29 family (miR-29a, b, and c) for just 1 wk is sufficient to enhance systemic insulin sensi-tivity in chow-fed lean mice and reduce fasting glucose levels in both chow-fed lean and HFD-fed obese mice. Hepatic *Dnmt3a* and *Enho* are among the candidate mediators identi-

Fig. 4. Identification of candidate mediators of the LNA29-mediated improvement in glycemic control. Enrichment analysis of miRNA target sites (using the Monte Carlo simulation tool miRhub) in genes upregulated (*A*) and downregulated (*B*) in the liver of fasted C57BL/6J mice by LNA29 (dashed line represents $P < 0.05$). The differentially expressed genes were identified by DESeq2 using cutoff $P < 0.05$ (Wald test), *P*-adj. < 0.2 (Benjamini-Hochberg method) and average base mean > 50. Saline, $n = 6$; LNA29, $n = 5$. *C*: Venn diagram showing the number of genes upregulated by LNA29 that have predicted target sites for miR-29. *D*: sequencing data of *Dnmt3a*, *Dnmt3b*, *Dgkd*, and *Enho* in the liver of fasted C57BL/6J mice treated with LNA29 compared with saline controls. *$*P < 0.05$ and ***$P < 0.001$ by Wald test (DESeq2). *E*: evolutionarily conserved miR-29 seed match sequence present in the 3′-UTR of *Enho* across multiple species. *F*: RT-qPCR of *ENHO* expression in Huh7 cells treated with transfection reagent alone or 200 nM of miR-29a inhibitor. Values are average from $n = 5$–6 wells per condition from 2 independent experiments. *$*P < 0.05$ by two-tailed Student's *t*-test. *G*: luciferase assays determining the effects of miR-29a mimic or miR-29a LNA on the activity of *ENHO* 3′-untranslated region (UTR) reported by firefly (FL) luciferase. The FL activity was normalized to Renilla (RL) luciferase activity. Values are average from $n = 6$ wells per condition from 2 independent experiments. *$*P < 0.05$ by two-tailed Student's *t*-test.
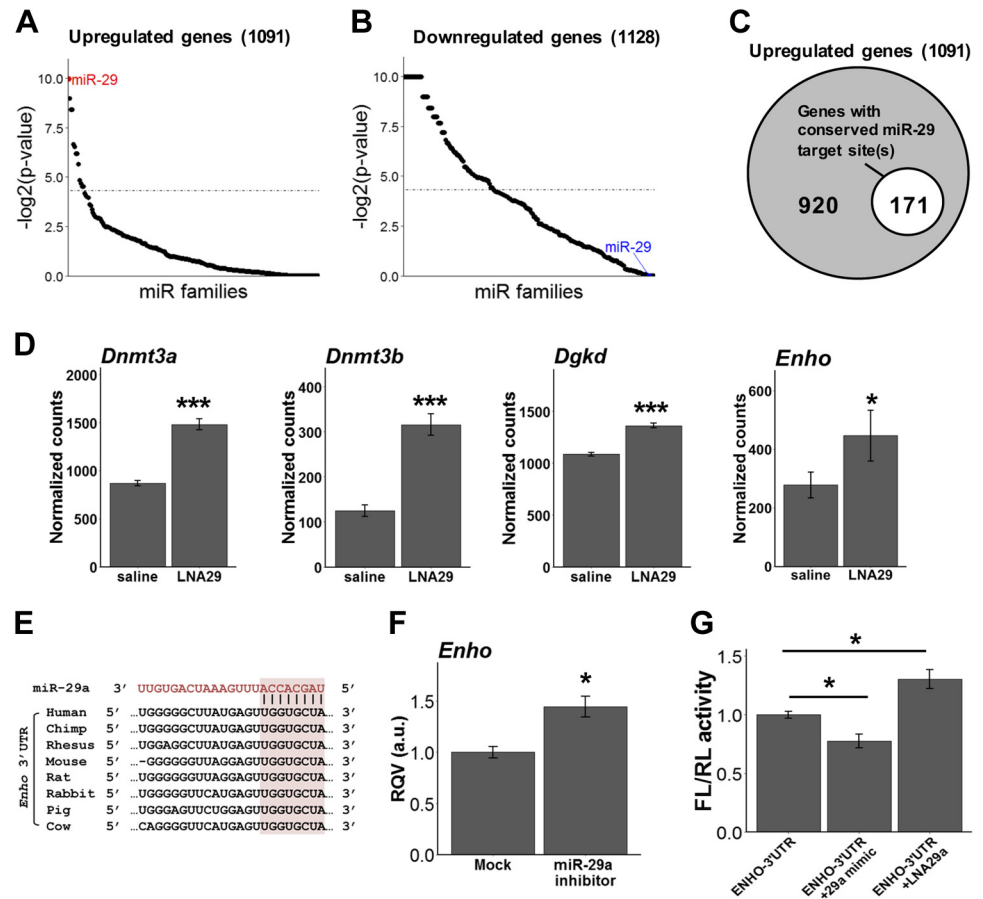
fied through our unbiased whole transcriptome study. The results generated in the present study lay a strong foundation for future investigations focused on testing the effects of LNA29 in additional diet-induced or genetic models of IR/T2D.

Several hepatic miRNAs that we identified as being dysregulated across multiple models of IR/T2D have been previously characterized to contribute to the development of IR/T2D in specific models. Those miRNAs include miR-802 (26), miR-107 (44), miR-34a (9), and miR-222 (37). Specifically, miR-802, miR-107, and miR-34a were observed to be elevated in the liver of diabetic mouse models compared with healthy lean controls, and pharmacological suppression of these miRNAs effectively ameliorates the IR phenotype in vivo (9, 26, 44). In addition, overexpression of miR-222 in primary mouse hepatocytes was recently shown to impair insulin signaling through inhibition of IRS-1 in vitro (37). Besides these previously characterized "diabeto-miRNAs," we identified a few additional miRNAs (miR-28 and miR-148b) that also appear to be commonly dysregulated across multiple models of IR/T2D. MiR-28 in the circulation has been shown to increase in obese T2D patients with uncharacterized mechanisms (21). MiR-148b has not been linked to IR-associated phenotype or metabolism, although the other member in this family, miR-148a, has been shown to be involved in the control of lipid metabolism and gluconeogenesis (17, 51). These miRNAs warrant further investigation to pinpoint their functional roles in the development and/or progression of IR/T2D.

In this study we also observed for the first time that hepatic miR-29b expression exhibits persistent dysregulation during diabetes progression in a relatively new disease model, the UCD-T2DM rat, which has never before been investigated for miRNA studies. The underlying mechanism by which hepatic miR-29b is dysregulated is not fully understood. We have previously reported that Foxa2 is upregulated in *fa/fa* diabetic rats and that transcription at both miR-29 loci is likely driven at least in part by Foxa2 in the liver (30). However, whether Foxa2 is responsible for the upregulation of miR-29 family members across different IR/T2D disease models is not known and merits further investigation. Notably, not all of the IR/T2D-associated hepatic miRNAs that we identified in the UCD-T2DM rats exhibit a similar behavior during the course of disease progression. While miR-107, miR-148b, and miR-222, together with miR-29b, exhibit persistent dysregulation over the course of diabetes progression, the expression levels of miR-802 and miR-34a actually decline in later stages. This could suggest that miR-802 and miR-34a are not necessary to drive disease progression after diabetes onset, but this hypothesis merits further investigation.

The link between hepatic miR-29 and systemic insulin sensitivity in vivo has been made once previously in genetic mouse models (13). There are major differences between this previously published work and our present study. In Dooley et al. (13), miR-29a$^{-/-}$ (global knockout of miR-29a/b-1 locus) and miR-29c$^{-/-}$ (global knockout of miR-29b-1/c locus) mice were generated to investigate miR-29 biology. MiR-29a$^{-/-}$

mice display a defect in insulin secretion that impairs hepatic glucose metabolism, whereas miR-29c$^{-/-}$ mice exhibit hepatic insulin hypersensitivity (13). Despite these important advances in knowledge, the physiological impact of acute suppression of the entire miR-29 family (miR-29a, b, and c) in the adult mouse was unknown. In this study, we bridge this important knowledge gap by using LNA technology in adult mice and show that 1 wk LNA-based suppression of the miR-29 family is sufficient to improve glycemic control in both chow-fed lean and HFD-fed obese mice. Also, it is important to note that Dooley et al. (13) actually observed an increase in fasting glucose in the miR-29a$^{-/-}$ mice, but this is mainly driven by a defect in insulin secretion from pancreatic islets. In our study, LNA29 exerts most of its effect in the liver, as the pancreas does not effectively take up LNA delivered by subcutaneous injection.

Previously we demonstrated that LNA29 treatment improves the circulating lipid profile (29). It is not yet known whether the effects of LNA29 on plasma lipid and glucose levels are mediated by the same mechanisms or whether the pathways are mutually exclusive. Nonetheless, these data open the question about the potential therapeutic value of LNA29 in animal models of IR/T2D. However, several facets of miR-29 biology and the open problem of effective tissue-specific LNA delivery methods need to be carefully considered. First, although no detrimental effects were observed in the chow-fed mice receiving one short-term dose of LNA29, the long-term effects of multiple doses of LNA29 need to be closely evaluated, particularly as it pertains to effects on extracellular matrix proteins and the development of fibrosis (46). Second, as indicated in our previous study (29), delivery of LNA29 by subcutaneous injection can diffuse to multiple tissue types besides the liver, and it is known that miR-29 has important functions in other tissues, including skeletal muscle (36). More work is required to establish tissue-specific delivery. It is important to note that, even aside from the potential future therapeutic potential, we believe this study is important from the standpoint of revealing new players in liver molecular networks that govern metabolic phenotypes, thereby advancing our understanding of the mechanisms used by the liver to regulate energy balance.

Hepatic *Dnmt3a* and *Enho* are identified as candidate mediators of LNA29 through our transcriptome study. Dnmt3a, which is a validated miR-29 target, has been linked to insulin sensitivity in multiple tissue/cell types such as adipose and neurons (25, 52). The increases in hepatic *Dnmt3a* by LNA29 at both RNA and protein levels motivate future studies of this potential mechanism in regulating hepatic insulin sensitivity. In addition, this is the first time that *Enho* has been implicated as a candidate miRNA-regulated gene. We are able to demonstrate using human cell lines that *Enho* is a direct target of miR-29. *Enho*, which is highly expressed in the liver and encodes energy homeostasis hormone Adropin, has been shown to regulate both insulin sensitivity and lipid homeostasis in rodent and nonhuman private models (5, 16, 28). Also, humans who carry *Enho* mutations have metabolic disorders (4, 6). It has been shown in mice that global genetic deficiency of *Enho* leads to dyslipidemia, obesity, and IR and that overexpression of *Enho* or systemic administration of Adropin in the chronic HFD condition significantly improves hepatic lipid homeostasis and insulin sensitivity (16, 28). We speculate that the upregulation of hepatic *Enho* by LNA29 may contribute to

the reduction of circulating lipids seen in our previous study (29), as well as the improvement of insulin sensitivity suggested in our present study. Future studies of LNA29 treatment in *Enho* knockout mice will help elucidate whether *Enho* is essential for mediating LNA29-induced beneficial effects.

Finally, this finding does not exclude the possibility that there are other potential mediators of the effects of LNA29; in fact, we fully anticipate that there are numerous other important direct and indirect targets of miR-29 that are pertinent to the improvements in glycemic control. For example, Insulin-Like Growth Factor Binding Protein 2 (*Igfbp2*) and apolipoprotein A-IV (*Apoa4*) are significantly upregulated by LNA29 in the liver of WT mice based on our RNA-Seq data (Fig. 4*C*; Supplementary Fig. S5, c and d). Several studies have proposed that Igfbp2 and Apoa4 are therapeutic targets for IR/T2D because of their roles in potentiating insulin signaling pathways or improving hepatic glucose metabolism (19, 33, 47). Igfbp2 is highly expressed in human liver, and low circulating Igfbp2 levels have been reported in multiple studies in humans with obesity and diabetes (15). Overexpression of Igfbp2 in mice mitigates HFD-induced obesity (47). ApoA-IV knockout mice exhibit an increase in hepatic glucose production, and the delivery of exogenous ApoA-IV protein lowers circulating glucose in mice (18, 34). Along these lines, the increase in *Igfbp2* and *Apoa4* by LNA29 may contribute to the improvement in systemic glycemic control. However, they are not predicted to be direct targets of miR-29; therefore, it is likely that their upregulation in response to LNA29 is indirect through specific transcription factors and/or RNA stabilizing binding proteins that may be directly regulated by miR-29.

In sum, we provide evidence from sequencing-based analysis of liver tissue from multiple rodent and monkey models of IR/T2D that hepatic miR-29b is strongly linked to hepatic IR irrespective of the underlying pathogenic mechanisms. Importantly, we use LNA technology to demonstrate that suppression of whole miR-29 family for only 1 wk is sufficient to enhance systemic insulin sensitivity in adult normoglycemic mice and reduce fasting glucose levels in HFD-fed obese mice.

DISCLOSURES

No conflicts of interest, financial or otherwise, are declared by the authors.

AUTHOR CONTRIBUTIONS

Y.-H.H. and P.S. conceived and designed research; Y.-H.H., C.L.K., R.C., R.P.B., J.M., L.Z., and J.L.G. performed experiments; Y.-H.H., M.K., C.L.K., R.P.B., J.M., and L.Z. analyzed data; Y.-H.H. interpreted results of experiments; Y.-H.H. and M.K. prepared figures; Y.-H.H. drafted manuscript; Y.-H.H. and P.S. edited and revised manuscript; Y.-H.H., M.K., C.L.K., M.M.H., P.J.H., S.B.B., P.J.W., and P.S. approved final version of manuscript.

REFERENCES

1. **Baran-Gale J, Fannin EE, Kurtz CL, Sethupathy P.** Beta cell 5′-shifted isomiRs are candidate regulatory hubs in type 2 diabetes. *PLoS One* 8: e73240, 2013. doi:10.1371/journal.pone.0073240.

2. **Belgardt BF, Ahmed K, Spranger M, Latreille M, Denzler R, Kondratiuk N, von Meyenn F, Villena FN, Herrmanns K, Bosco D, Kerr-Conte J, Pattou F, Rülicke T, Stoffel M.** The microRNA-200 family regulates pancreatic beta cell survival in type 2 diabetes. *Nat Med* 21: 619–627, 2015. doi:10.1038/nm.3862.

3. **Bremer AA, Stanhope KL, Graham JL, Cummings BP, Ampah SB, Saville BR, Havel PJ.** Fish oil supplementation ameliorates fructose-induced hypertriglyceridemia and insulin resistance in adult male rhesus macaques. *J Nutr* 144: 5–11, 2014. doi:10.3945/jn.113.178061.

4. **Butler AA, Tam CS, Stanhope KL, Wolfe BM, Ali MR, O'Keeffe M, St-Onge MP, Ravussin E, Havel PJ.** Low circulating adropin concentrations with obesity and aging correlate with risk factors for metabolic disease and increase after gastric bypass surgery in humans. *J Clin Endocrinol Metab* 97: 3783–3791, 2012. doi:10.1210/jc.2012-2194.

5. **Butler AA, Zhang J, Price CA, Stevens JR, Graham JL, Stanhope KL, King S, Krauss RM, Bremer AA, Havel PJ.** Low plasma adropin concentrations increase risks of weight gain and metabolic dysregulation in response to a high-sugar diet in male nonhuman primates. *J Biol Chem* 294: 9706–9719, 2019. doi:10.1074/jbc.RA119.007528.

6. **Chen S, Zeng K, Liu QC, Guo Z, Zhang S, Chen XR, Lin JH, Wen JP, Zhao CF, Lin XH, Gao F.** Adropin deficiency worsens HFD-induced metabolic defects. *Cell Death Dis* 8: e3008, 2017. doi:10.1038/cddis.2017.362.

7. **Cheng L, Zhu Y, Han H, Zhang Q, Cui K, Shen H, Zhang J, Yan J, Prochownik E, Li Y.** MicroRNA-148a deficiency promotes hepatic lipid metabolism and hepatocarcinogenesis in mice. *Cell Death Dis* 8: e2916, 2017. doi:10.1038/cddis.2017.309.

8. **Chibalin AV, Leng Y, Vieira E, Krook A, Björnholm M, Long YC, Kotova O, Zhong Z, Sakane F, Steiler T, Nylén C, Wang J, Laakso M, Topham MK, Gilbert M, Wallberg-Henriksson H, Zierath JR.** Down-regulation of diacylglycerol kinase delta contributes to hyperglycemia-induced insulin resistance. *Cell* 132: 375–386, 2008. doi:10.1016/j.cell.2007.12.035.

9. **Choi SE, Fu T, Seok S, Kim DH, Yu E, Lee KW, Kang Y, Li X, Kemper B, Kemper JK.** Elevated microRNA-34a in obesity reduces NAD+ levels and SIRT1 activity by directly targeting NAMPT. *Aging Cell* 12: 1062–1072, 2013. doi:10.1111/acel.12135.

10. **Cummings BP, Digitale EK, Stanhope KL, Graham JL, Baskin DG, Reed BJ, Sweet IR, Griffen SC, Havel PJ.** Development and characterization of a novel rat model of type 2 diabetes mellitus: the UC Davis type 2 diabetes mellitus UCD-T2DM rat. *Am J Physiol Regul Integr Comp Physiol* 295: R1782–R1793, 2008. doi:10.1152/ajpregu.90635.2008.

11. **Davegårdh C, García-Calzón S, Bacos K, Ling C.** DNA methylation in the pathogenesis of type 2 diabetes in humans. *Mol Metab* 14: 12–25, 2018. doi:10.1016/j.molmet.2018.01.022.

12. **Dobin A, Davis CA, Schlesinger F, Drenkow J, Zaleski C, Jha S, Batut P, Chaisson M, Gingeras TR.** STAR: ultrafast universal RNA-seq aligner. *Bioinformatics* 29: 15–21, 2013. doi:10.1093/bioinformatics/bts635.

13. **Dooley J, Garcia-Perez JE, Sreenivasan J, Schlenner SM, Vangoitsenhoven R, Papadopoulou AS, Tian L, Schonefeldt S, Serneels L, Deroose C, Staats KA, Van der Schueren B, De Strooper B, McGuinness OP, Mathieu C, Liston A.** The microRNA-29 Family Dictates the Balance Between Homeostatic and Pathological Glucose Handling in Diabetes and Obesity. *Diabetes* 65: 53–61, 2016. doi:10.2337/db15-0770.

14. **Fabbri M, Garzon R, Cimmino A, Liu Z, Zanesi N, Callegari E, Liu S, Alder H, Costinean S, Fernandez-Cymering C, Volinia S, Guler G, Morrison CD, Chan KK, Marcucci G, Calin GA, Huebner K, Croce CM.** MicroRNA-29 family reverts aberrant methylation in lung cancer by targeting DNA methyltransferases 3A and 3B. *Proc Natl Acad Sci USA* 104: 15805–15810, 2007. doi:10.1073/pnas.0707628104.

15. **Frystyk J, Skjaerbaek C, Vestbo E, Fisker S, Orskov H.** Circulating levels of free insulin-like growth factors in obese subjects: the impact of type 2 diabetes. *Diabetes Metab Res Rev* 15: 314–322, 1999. doi:10.1002/(SICI)1520-7560(199909/10)15:5<314:AID-DMRR56>3.0.CO;2-E.

16. **Ganesh Kumar K, Zhang J, Gao S, Rossi J, McGuinness OP, Halem HH, Culler MD, Mynatt RL, Butler AA.** Adropin deficiency is associated with increased adiposity and insulin resistance. *Obesity (Silver Spring)* 20: 1394–1402, 2012. doi:10.1038/oby.2012.31.

17. **Goedeke L, Rotllan N, Canfrán-Duque A, Aranda JF, Ramírez CM, Araldi E, Lin CS, Anderson NN, Wagschal A, de Cabo R, Horton JD, Lasunción MA, Näär AM, Suárez Y, Fernández-Hernando C.** MicroRNA-148a regulates LDL receptor and ABCA1 expression to control circulating lipoprotein levels. *Nat Med* 21: 1280–1289, 2015. doi:10.1038/nm.3949.

18. **Heald AH, Kaushal K, Siddals KW, Rudenski AS, Anderson SG, Gibson JM.** Insulin-like growth factor binding protein-2 (IGFBP-2) is a marker for the metabolic syndrome. *Exp Clin Endocrinol Diabetes* 114: 371–376, 2006. doi:10.1055/s-2006-924320.

19. **Hoeflich A, Wu M, Mohan S, Föll J, Wanke R, Froehlich T, Arnold GJ, Lahm H, Kolb HJ, Wolf E.** Overexpression of insulin-like growth factor-binding protein-2 in transgenic mice reduces postnatal body weight gain. *Endocrinology* 140: 5488–5496, 1999. doi:10.1210/endo.140.12.7169.

20. **Hu W, Dooley J, Chung SS, Chandramohan D, Cimmino L, Mukherjee S, Mason CE, de Strooper B, Liston A, Park CY.** miR-29a maintains mouse hematopoietic stem cell self-renewal by regulating Dnmt3a. *Blood* 125: 2206–2216, 2015. doi:10.1182/blood-2014-06-585273.

21. **Jones A, Danielson KM, Benton MC, Ziegler O, Shah R, Stubbs RS, Das S, Macartney-Coxson D.** miRNA Signatures of Insulin Resistance in Obesity. *Obesity (Silver Spring)* 25: 1734–1744, 2017. doi:10.1002/oby.21950.

22. **Kanke M, Baran-Gale J, Villanueva J, Sethupathy P.** miRquant 2.0: an Expanded Tool for Accurate Annotation and Quantification of MicroRNAs and their isomiRs from Small RNA-Sequencing Data. *J Integr Bioinform* 13: 307, 2016. doi:10.1515/jib-2016-307.

23. **Karolina DS, Armugam A, Tavintharan S, Wong MT, Lim SC, Sum CF, Jeyaseelan K.** MicroRNA 144 impairs insulin signaling by inhibiting the expression of insulin receptor substrate 1 in type 2 diabetes mellitus. *PLoS One* 6: e22839, 2011. [Erratum in *PLoS One* 6: 2011] doi:10.1371/journal.pone.0022839.

24. **Kleinert M, Clemmensen C, Hofmann SM, Moore MC, Renner S, Woods SC, Huypens P, Beckers J, de Angelis MH, Schürmann A, Bakhti M, Klingenspor M, Heiman M, Cherrington AD, Ristow M, Lickert H, Wolf E, Havel PJ, Müller TD, Tschöp MH.** Animal models of obesity and diabetes mellitus. *Nat Rev Endocrinol* 14: 140–162, 2018. doi:10.1038/nrendo.2017.161.

25. **Kohno D, Lee S, Harper MJ, Kim KW, Sone H, Sasaki T, Kitamura T, Fan G, Elmquist JK.** Dnmt3a in Sim1 neurons is necessary for normal energy homeostasis. *J Neurosci* 34: 15288–15296, 2014. doi:10.1523/JNEUROSCI.1316-14.2014.

26. **Kornfeld JW, Baitzel C, Könner AC, Nicholls HT, Vogt MC, Herrmanns K, Scheja L, Haumaitre C, Wolf AM, Knippschild U, Seibler J, Cereghini S, Heeren J, Stoffel M, Brüning JC.** Obesity-induced overexpression of miR-802 impairs glucose metabolism through silencing of Hnf1b. *Nature* 494: 111–115, 2013. doi:10.1038/nature11793.

27. **Kriegel AJ, Liu Y, Fang Y, Ding X, Liang M.** The miR-29 family: genomics, cell biology, and relevance to renal and cardiovascular injury. *Physiol Genomics* 44: 237–244, 2012. doi:10.1152/physiolgenomics.00141.2011.

28. **Kumar KG, Trevaskis JL, Lam DD, Sutton GM, Koza RA, Chouljenko VN, Kousoulas KG, Rogers PM, Kesterson RA, Thearle M, Ferrante AW Jr, Mynatt RL, Burris TP, Dong JZ, Halem HA, Culler MD, Heisler LK, Stephens JM, Butler AA.** Identification of adropin as a secreted factor linking dietary macronutrient intake with energy homeostasis and lipid metabolism. *Cell Metab* 8: 468–481, 2008. doi:10.1016/j.cmet.2008.10.011.

29. **Kurtz CL, Fannin EE, Toth CL, Pearson DS, Vickers KC, Sethupathy P.** Inhibition of miR-29 has a significant lipid-lowering benefit through suppression of lipogenic programs in liver. *Sci Rep* 5: 12911, 2015. doi:10.1038/srep12911.

30. **Kurtz CL, Peck BC, Fannin EE, Beysen C, Miao J, Landstreet SR, Ding S, Turaga V, Lund PK, Turner S, Biddinger SB, Vickers KC, Sethupathy P.** MicroRNA-29 fine-tunes the expression of key FOXA2-activated lipid metabolism genes and is dysregulated in animal models of insulin resistance and diabetes. *Diabetes* 63: 3141–3148, 2014. doi:10.2337/db13-1015.

31. **Latreille M, Hausser J, Stützer I, Zhang Q, Hastoy B, Gargani S, Kerr-Conte J, Pattou F, Zavolan M, Esguerra JL, Eliasson L, Rülicke**

T, Rorsman P, Stoffel M. MicroRNA-7a regulates pancreatic β cell function. *J Clin Invest* 124: 2722–2735, 2014. doi:10.1172/JCI73066.

32. Lawan A, Min K, Zhang L, Canfran-Duque A, Jurczak MJ, Campo-rez JPG, Nie Y, Gavin TP, Shulman GI, Fernandez-Hernando C, Bennett AM. Skeletal Muscle-Specific Deletion of MKP-1 Reveals a p38 MAPK/JNK/Akt Signaling Node That Regulates Obesity-Induced Insulin Resistance. *Diabetes* 67: 624–635, 2018. doi:10.2337/db17-0826.

33. Li X, Wang F, Xu M, Howles P, Tso P. ApoA-IV improves insulin sensitivity and glucose uptake in mouse adipocytes via PI3K-Akt Signaling. *Sci Rep* 7: 41289, 2017. doi:10.1038/srep41289.

34. Li X, Xu M, Wang F, Kohan AB, Haas MK, Yang Q, Lou D, Obici S, Davidson WS, Tso P. Apolipoprotein A-IV reduces hepatic gluconeo-genesis through nuclear receptor NR1D1. *J Biol Chem* 289: 2396–2404, 2014. doi:10.1074/jbc.M113.511766.

35. Love MI, Huber W, Anders S. Moderated estimation of fold change and dispersion for RNA-seq data with DESeq2. *Genome Biol* 15: 550, 2014. doi:10.1186/s13059-014-0550-8.

36. Massart J, Sjögren RJO, Lundell LS, Mudry JM, Franck N, O'Gorman DJ, Egan B, Zierath JR, Krook A. Altered miR-29 Expres-sion in Type 2 Diabetes Influences Glucose and Lipid Metabolism in Skeletal Muscle. *Diabetes* 66: 1807–1818, 2017. doi:10.2337/db17-0141.

37. Ono K, Igata M, Kondo T, Kitano S, Takaki Y, Hanatani S, Sakaguchi M, Goto R, Senokuchi T, Kawashima J, Furukawa N, Motoshima H, Araki E. Identification of microRNA that represses IRS-1 expression in liver. *PLoS One* 13: e0191553, 2018. doi:10.1371/journal.pone.0191553.

38. Patro R, Duggal G, Love MI, Irizarry RA, Kingsford C. Salmon provides fast and bias-aware quantification of transcript expression. *Nat Methods* 14: 417–419, 2017. doi:10.1038/nmeth.4197.

39. Poy MN, Hausser J, Trajkovski M, Braun M, Collins S, Rorsman P, Zavolan M, Stoffel M. miR-375 maintains normal pancreatic alpha- and beta-cell mass. *Proc Natl Acad Sci USA* 106: 5813–5818, 2009. doi:10.1073/pnas.0810550106.

40. Selitsky SR, Dinh TA, Toth CL, Kurtz CL, Honda M, Struck BR, Kaneko S, Vickers KC, Lemon SM, Sethupathy P. Transcriptomic Analysis of Chronic Hepatitis B and C and Liver Cancer Reveals Mi-croRNA-Mediated Control of Cholesterol Synthesis Programs. *MBio* 6: e01500–e01515, 2015. doi:10.1128/mBio.01500-15.

41. Smith SS, Kessler CB, Shenoy V, Rosen CJ, Delany AM. IGF-I 3′ untranslated region: strain-specific polymorphisms and motifs regulating IGF-I in osteoblasts. *Endocrinology* 154: 253–262, 2013. doi:10.1210/en.2012-1476.

42. Thomou T, Mori MA, Dreyfuss JM, Konishi M, Sakaguchi M, Wol-frum C, Rao TN, Winnay JN, Garcia-Martin R, Grinspoon SK, Gorden P, Kahn CR. Adipose-derived circulating miRNAs regulate gene expression in other tissues. *Nature* 542: 450–455, 2017. [Erratum in *Nature* 545: 252, 2017] doi:10.1038/nature21365.

43. Torella D, Iaconetti C, Tarallo R, Marino F, Giurato G, Veneziano C, Aquila I, Scalise M, Mancuso T, Cianflone E, Valeriano C, Marotta P, Tamme L, Vicinanza C, Sasso FC, Cozzolino D, Torella M, Weisz A, Indolfi C. miRNA Regulation of the Hyperproliferative Phenotype of Vascular Smooth Muscle Cells in Diabetes. *Diabetes* 67: 2554–2568, 2018. doi:10.2337/db17-1434.

44. Trajkovski M, Hausser J, Soutschek J, Bhat B, Akin A, Zavolan M, Heim MH, Stoffel M. MicroRNAs 103 and 107 regulate insulin sensi-tivity. *Nature* 474: 649–653, 2011. doi:10.1038/nature10112.

45. Vega-Badillo J, Gutiérrez-Vidal R, Hernández-Pérez HA, Villamil-Ramírez H, León-Mimila P, Sánchez-Muñoz F, Morán-Ramos S, Larrieta-Carrasco E, Fernández-Silva I, Méndez-Sánchez N, Tovar AR, Campos-Pérez F, Villarreal-Molina T, Hernández-Pando R, Aguilar-Salinas CA, Canizales-Quinteros S. Hepatic miR-33a/miR-144 and their target gene ABCA1 are associated with steatohepatitis in mor-bidly obese subjects. *Liver Int* 36: 1383–1391, 2016. doi:10.1111/liv.13109.

46. Wang J, Chu ES, Chen HY, Man K, Go MY, Huang XR, Lan HY, Sung JJ, Yu J. microRNA-29b prevents liver fibrosis by attenuating hepatic stellate cell activation and inducing apoptosis through targeting PI3K/AKT pathway. *Oncotarget* 6: 7325–7338, 2015. doi:10.18632/oncotarget.2621.

47. Wheatcroft SB, Kearney MT, Shah AM, Ezzat VA, Miell JR, Modo M, Williams SC, Cawthorn WP, Medina-Gomez G, Vidal-Puig A, Sethi JK, Crossey PA. IGF-binding protein-2 protects against the devel-opment of obesity and insulin resistance. *Diabetes* 56: 285–294, 2007. doi:10.2337/db06-0436.

48. White PJ, McGarrah RW, Grimsrud PA, Tso SC, Yang WH, Halde-man JM, Grenier-Larouche T, An J, Lapworth AL, Astapova I, Hannou SA, George T, Arlotto M, Olson LB, Lai M, Zhang GF, Ilkayeva O, Herman MA, Wynn RM, Chuang DT, Newgard CB. The BCKDH Kinase and Phosphatase Integrate BCAA and Lipid Metabolism via Regulation of ATP-Citrate Lyase. *Cell Metab* 27: 1281–1293.e1287, 2018.

49. Xie H, Lim B, Lodish HF. MicroRNAs induced during adipogenesis that accelerate fat cell development are downregulated in obesity. *Diabetes* 58: 1050–1057, 2009. doi:10.2337/db08-1299.

50. Yakar S, Liu JL, Fernandez AM, Wu Y, Schally AV, Frystyk J, Chernausek SD, Mejia W, Le Roith D. Liver-specific igf-1 gene deletion leads to muscle insulin insensitivity. *Diabetes* 50: 1110–1118, 2001. doi:10.2337/diabetes.50.5.1110.

51. Yan X, Wang Z, Bishop CA, Weitkunat K, Feng X, Tarbier M, Luo J, Friedländer MR, Burkhardt R, Klaus S, Willnow TE, Poy MN. Control of hepatic gluconeogenesis by Argonaute2. *Mol Metab* 18: 15–24, 2018. doi:10.1016/j.molmet.2018.10.003.

52. You D, Nilsson E, Tenen DE, Lyubetskaya A, Lo JC, Jiang R, Deng J, Dawes BA, Vaag A, Ling C, Rosen ED, Kang S. Dnmt3a is an epigenetic mediator of adipose insulin resistance. *eLife* 6: e30766, 2017. doi:10.7554/eLife.30766.